Eigenmodes of a reflective twisted-nematic liquid-crystal cell

Xinyu Zhu, Qi Hong, Yuhua Huang, and Shin-Tson Wu[a)]
School of Optics/CREOL, University of Central Florida, Orlando, Florida 32816-2700

(Received 3 April 2003; accepted 4 June 2003)

The eigenmodes of a reflective twisted-nematic liquid-crystal (TN LC) cell are analyzed based on the Jones matrix method. Two models are developed to describe the LC system in the low- and high-voltage regimes. The simulated transmission spectra of LC Fabry–Perot etalons are used to investigate the eigenmodes. In a general reflective TN LC cell, the eigenmodes are two orthogonal linear polarization states. Under some specific conditions, these two linear polarization states will approach the bisector or orthogonal to the bisector of the TN LC cell. This bisector effect is useful for reducing the operating voltage and enhancing the contrast ratio of LC display devices and for eliminating the mode coupling of the tunable Fabry–Perot etalons. © *2003 American Institute of Physics.* [DOI: 10.1063/1.1595145]

I. INTRODUCTION

Twisted-nematic liquid-crystal (TN LC) cell has been widely employed in transmissive and reflective displays.[1,2] The reflective liquid-crystal display (LCD) has advantages over the transmission type in sunlight readability, low-power consumption, and light weight due to the elimination of backlight. Several single-polarizer-based reflective LCD modes have been developed; for example, the TN electrically controlled birefringence mode,[3] the mixed TN mode,[4] and the self-compensated TN mode.[5] These modes can be used in both direct-view and projection displays.

For display applications, if the incident light happens to be at the bisector of the LC twist angle,[6] a good dark state can be achieved at a relatively low voltage, although the color dispersion is increased. Low operating voltage leads to a low power consumption, which is particularly desirable for handheld display devices aiming for mobile communications. In addition, for a tunable LC Fabry–Perot (FP) etalon intended for telecom application,[7] only those eigenmodes resonating in the FP cavity can be amplified. To eliminate the mode coupling, the incident light is preferred to be an eigenmode. Therefore, for the interest of optimizing the LC operation for displays and tunable FP filters, it is essential to thoroughly analyze the bisector effect and the eigenmodes of the reflective TN cell.

In this article, we will first derive the eigenmodes of a general reflective TN LC cell at null-voltage and high-voltage states based on the Jones matrix method.[8] Next, some simulation results are given to illuminate these eigenmodes using the transmission spectra of the TN-LC-based FP etalons.

II. EIGENMODE DERIVATION

A. Uniform twist model

For a reflective TN LC cell with a twist angle ϕ, the LC directors[9] twist uniformly throughout the cell when no voltage is applied. We call this a uniform twist model. If an input polarized light happens to be an eigenmode, then after a round trip, the polarization transformation should be

$$\gamma\mathbf{E}=\mathbf{R}(-\phi)\mathbf{J}(-\phi)\mathbf{R}(\phi)\mathbf{J}(\phi)\mathbf{E}, \tag{1}$$

where $\mathbf{E}=(E_x,E_y)^T$ is the vector describing the input light polarization, γ is the eigenvalue of the round-trip transmission matrices, and

$$\mathbf{J}(\phi)=\mathbf{R}(-\phi)\times\begin{pmatrix}\cos X-i\frac{\Gamma}{2}\frac{\sin X}{X} & \phi\frac{\sin X}{X}\\ -\Phi\frac{\sin X}{X} & \cos X+i\frac{\Gamma}{2}\frac{\sin X}{X}\end{pmatrix} \tag{2}$$

is the Jones matrix of the uniformly twisted TN LC.[8] $\mathbf{R}(\phi)$ is the coordinates rotation matrix, which has the following form:

$$\mathbf{R}(\phi)=\begin{pmatrix}\cos\phi & \sin\phi\\ -\sin\phi & \cos\phi\end{pmatrix}. \tag{3}$$

In Eq. (2), $\Gamma=2\pi d\Delta n/\lambda$ is the phase retardation of the TN LC layer, $X=\sqrt{\phi^2+(\Gamma/2)^2}$; d is the LC cell gap, Δn the LC birefringence, and λ the incident light wavelength. In the coordinate system shown in Eq. (1), we define the x-axis to be parallel to the direction of the entrance surface director, that is, the rubbing direction of the entrance substrate. In addition, all of the angles are defined to be positive for the counterclockwise direction and negative for the clockwise direction with reference to the x-axis.

By solving Eq. (1), we obtain the eigenvalues as

$$\gamma_{\pm}=1-2\left(\frac{\Gamma}{2}\frac{\sin X}{X}\right)^2\pm i2\left(\frac{\Gamma}{2}\frac{\sin X}{X}\right)\sqrt{1-\left(\frac{\Gamma}{2}\frac{\sin X}{X}\right)^2}, \tag{4}$$

where the subscript "±" denotes different eigenvalues. In order to get the corresponding eigenmodes, one can substitute these two complex eigenvalues into Eq. (1) and derive the following equation:

a)Electronic mail: swu@mail.ucf.edu

$$\left(\frac{\Gamma}{2}\frac{\sin X}{X}\right)\begin{bmatrix} -\cos X \mp \sqrt{1-\left(\frac{\Gamma}{2}\frac{\sin X}{X}\right)^2} & -\phi\frac{\sin X}{X} \\ -\phi\frac{\sin X}{X} & \cos X \mp \sqrt{1-\left(\frac{\Gamma}{2}\frac{\sin X}{X}\right)^2} \end{bmatrix}\begin{pmatrix} E_x \\ E_y \end{pmatrix} = \begin{pmatrix} 0 \\ 0 \end{pmatrix}. \tag{5}$$

Equation (5) represents the general solutions for the eigenmodes of a reflective TN LC cell. First, let us discuss the eigenmodes for the following four cases.

1. When $\Gamma=0$ (isotropic media or vertically aligned nematic LC) or $\sin X=0$ (Gooch–Tarry minima conditions),[10] Eq. (5) is simplified to

$$\begin{pmatrix} 0 & 0 \\ 0 & 0 \end{pmatrix}\begin{pmatrix} E_x \\ E_y \end{pmatrix} = \begin{pmatrix} 0 \\ 0 \end{pmatrix}. \tag{6}$$

Under such a circumstance, the eigenmodes are any two orthogonal polarization states.

2. When $\phi=0$ (nontwist alignment), Eq. (5) is simplified as

$$\sin\frac{\Gamma}{2}\begin{pmatrix} -\cos\frac{\Gamma}{2} \mp \cos\frac{\Gamma}{2} & 0 \\ 0 & \cos\frac{\Gamma}{2} \mp \cos\frac{\Gamma}{2} \end{pmatrix}\begin{pmatrix} E_x \\ E_y \end{pmatrix} = \begin{pmatrix} 0 \\ 0 \end{pmatrix}. \tag{7}$$

In this case, the eigenmodes are the two linear polarization states parallel $[(1,0)^T]$ and perpendicular $[(0,1)^T]$ to the x-axis.

3. When $\Gamma/2 \gg \phi$ (Mauguin limit for the waveguiding effect to occur), then $X \approx \Gamma/2$ and $\phi/X \approx 0$. Under such a circumstance, Eq. (5) is reduced to

$$\sin\frac{\Gamma}{2}\begin{pmatrix} -\cos\frac{\Gamma}{2} \mp \cos\frac{\Gamma}{2} & 0 \\ 0 & \cos\frac{\Gamma}{2} \mp \cos\frac{\Gamma}{2} \end{pmatrix}\begin{pmatrix} E_x \\ E_y \end{pmatrix} = \begin{pmatrix} 0 \\ 0 \end{pmatrix}. \tag{8}$$

Similar to the case of $\phi=0$, the eigenmodes are the two linear polarization states parallel $[(1,0)^T]$ and perpendicular $[(0,1)^T]$ to the x-axis.

4. In a general case of a reflective TN LC cell, assuming $E_x=1$, the y-components of the eigenmodes, according to Eq. (5), are expressed as

$$E_{y,\pm} = \frac{\cos X \pm \sqrt{1-\left(\frac{\Gamma}{2}\frac{\sin X}{X}\right)^2}}{\phi\frac{\sin X}{X}}, \tag{9}$$

where the subscripts "$\pm$" in Eq. (9) denote different eigenmodes. We notice that $E_{y,\pm}$ is always real, which means in a general case the eigenmodes of a reflective TN LC cell are always linearly polarized, independent of ϕ and Γ. Besides, Eq. (9) indicates that these two eigenmodes are always orthogonal since $E_{x,+}E_{x,-}+E_{y,+}E_{y,-}=0$. Particularly, if $\Gamma/2 \ll \phi$ (i.e., $d\Delta n/\lambda \ll \phi/\pi$), then $\phi \approx X$ and $(\Gamma/2)/X \approx 0$, and Eq. (9) can be approximated as

$$E_{y,\pm} \approx -\frac{\cos\phi \pm 1}{\sin\phi} = \begin{cases} \tan(\phi/2+\pi/2) & \text{for "+" sign} \\ \tan(\phi/2) & \text{for "−" sign} \end{cases}. \tag{10}$$

When the condition that $d\Delta n/\lambda \ll \phi/\pi$ holds, one of the eigenmodes is parallel to the bisector of the twist angle and the other is perpendicular to the bisector. This is the bisector effect of the reflective TN cell we discuss in this article. The bisector effect leads to a low operating voltage for display applications.[11] This is particularly important for a projection display, in which low voltage helps to minimize the undesirable fringing field effect which, in turn, degrades the contrast ratio.[12]

B. Boundary layers model

In a high-voltage state, the bulk LC directors are reoriented to be along the electric field direction, except that the boundary layers remain undisturbed because of the strong surface anchoring.[13] The whole TN LC cell can be treated as two symmetric uniaxial birefringence layers oriented at an angle ϕ. We call this configuration the boundary layers model.

The residual phase difference ψ of each boundary layer is related to the applied voltage; as the applied voltage increases, the residual phase is gradually decreased. If the incident polarized light happens to be an eigenmode, then after a round-trip propagation the polarization transformation can be expressed as

$$\gamma\mathbf{E} = \mathbf{TR}(-\phi)\mathbf{T}^2\mathbf{R}(\phi)\mathbf{TE}, \tag{11}$$

where $\mathbf{E}=(E_x,E_y)^T$ is the vector describing the input light polarization, γ is the eigenvalue of the round-trip transmission matrices, $\mathbf{R}(\phi)$ is the rotation matrix as expressed in Eq. (3), and

$$\mathbf{T} = \begin{bmatrix} \exp(-i\psi/2) & 0 \\ 0 & \exp(i\psi/2) \end{bmatrix} \tag{12}$$

is the Jones matrix of each uniaxial boundary layer.

By solving Eq. (11), we obtain two eigenvalues:

$$\gamma_\pm = B \pm i\sqrt{1-B^2}, \tag{13}$$

where $B=\sin^2\phi+\cos^2\phi\cos 2\psi$. Note that $B \leqslant 1$. After substituting the eigenvalues into Eq. (11), we get the following equation for determining the corresponding eigenmodes:

$$\cos\phi\sin\psi\begin{pmatrix} -\cos\psi\cos\phi\mp\sqrt{\cos^2\phi\cos^2\psi+\sin^2\phi} & -\sin\phi \\ -\sin\phi & \cos\psi\cos\phi\mp\sqrt{\cos^2\phi\cos^2\psi+\sin^2\phi}\end{pmatrix}\begin{pmatrix}E_x\\E_y\end{pmatrix}=\begin{pmatrix}0\\0\end{pmatrix}. \tag{14}$$

Based on Eq. (14), we discuss three cases.

1. When $\sin\psi=0$ (isotropic media or vertical alignment) or $\cos\phi=0$ (twist angle $\phi=(2n+1)\pi/2$, where n is an integer), Eq. (14) is simplified as

$$\begin{pmatrix}0 & 0\\0 & 0\end{pmatrix}\begin{pmatrix}E_x\\E_y\end{pmatrix}=\begin{pmatrix}0\\0\end{pmatrix}. \tag{15}$$

In these cases, the eigenmodes are any two orthogonal polarization states. It is obvious that any normal incident polarized light experiences no phase difference in isotropic media, vertical aligned LC, or two orthogonal uniaxial layers with identical phase retardation. In these cases, any two orthogonally polarized lights can be the eigenmodes.

2. When $\phi=0$ (nontwist alignment), Eq. (14) has following form:

$$\sin\psi\begin{pmatrix}-\cos\psi\mp\cos\psi & 0\\0 & \cos\psi\mp\cos\psi\end{pmatrix}\begin{pmatrix}E_x\\E_y\end{pmatrix}=\begin{pmatrix}0\\0\end{pmatrix}. \tag{16}$$

Equation (16) is actually equivalent to Eq. (7) since ψ only counts for the phase retardation of a boundary layer. Thus, $\psi=\Gamma/2$. In this case, the eigenmodes are the two linear polarization states parallel $[(1,0)^T]$ and perpendicular $[(0,1)^T]$ to the x-axis.

3. In the general case of a reflective TN LC cell, let us assume $E_x=1$, then the y-components of the eigenmodes can be solved from Eq. (14):

$$E_{y,\pm}=\frac{\cos\psi\cos\phi\pm\sqrt{\cos^2\phi\cos^2\psi+\sin^2\phi}}{\sin\phi}. \tag{17}$$

Similar to the aforementioned uniform-twist model, the eigenmodes in the boundary layers model are also two orthogonal linear polarization states, independent of ϕ and ψ. Particularly, when the applied voltage is sufficiently large, the phase retardation of each boundary uniaxial layer is so small that $\psi\to0$. Thus, Eq. (17) can be approximated as

$$E_{y,\pm}\approx-\frac{\cos\phi\pm1}{\sin\phi}=\begin{cases}\tan(\phi/2+\pi/2) & \text{for ``+'' sign}\\ \tan(\phi/2) & \text{for ``-'' sign}\end{cases}. \tag{18}$$

In a high-voltage state ($V\gg V_{\rm th}$, where $V_{\rm th}$ is the threshold voltage of the reflective TN LC cell), the residual phase retardation is very small and the two eigenmodes are the two linear polarization states nearly parallel and perpendicular to the bisector of the twist angle.

From these analyses, we find that the eigenmodes of a general reflective TN LC cell are the two orthogonal linear polarization states. One of these two linear polarization states is the bisector and the other is orthogonal to the bisector, provided that the condition $\Gamma/2\ll\phi$ is satisfied, even without applied voltage. In a high-voltage state, these two linear polarization states also approach the bisector (or its perpendicular direction) when the residual phase of each boundary layer is close to 0.

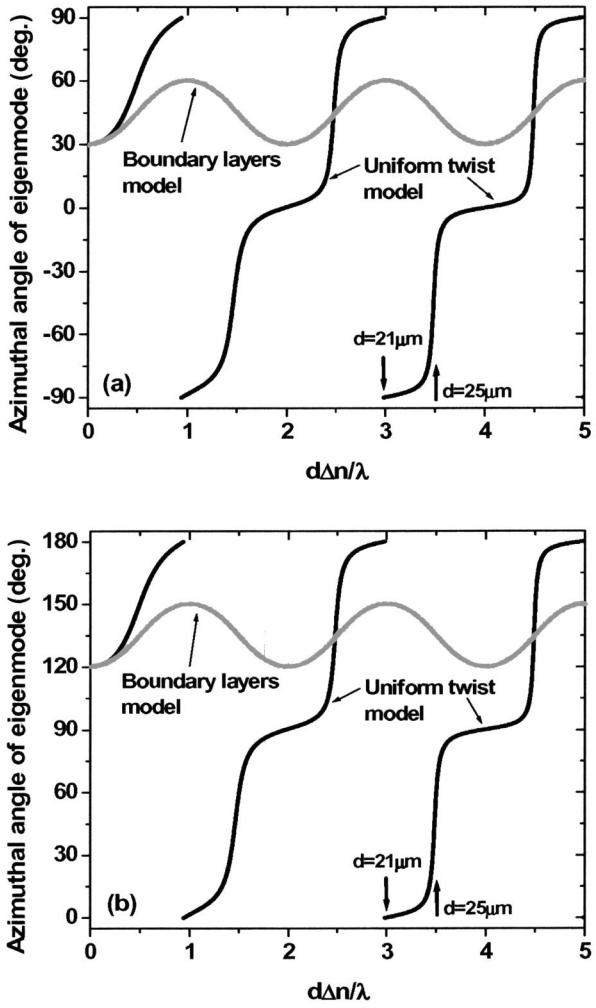

FIG. 1. The relationship between the azimuthal angles of the eigenmodes and $d\Delta n/\lambda$ for a 60° reflective TN LC cell. (a) The first eigenmode and (b) the second eigenmode. Here, only the general cases are considered according to Eqs. (9) and (17), and the azimuthal angle of eigenmode is obtained from $\arctan(E_{y,\pm}/E_x)$.

To illustrate the relationship between the azimuthal angles of the eigenmodes and the phase retardation of the TN LC discussed earlier, we chose a 60° reflective TN LC cell as an example. Figure 1 shows the dependence of the azimuthal angles of the eigenmodes on $d\Delta n/\lambda$ under the two models described in Eqs. (9) and (17). Here, the azimuthal angle is the tangential angle of the linearly polarized light obtained from $\arctan(E_{y,\pm}/E_x)$. It should be pointed out that the azimuthal angle has a period of 180°. From Fig. 1, the calculated results from the uniform twist model are generally quite different from those from the boundary layers model, except for some intersections. As the $d\Delta n/\lambda$ decreases to ~0.2, these two results gradually merge. With further reduction in

$d\Delta n/\lambda$, the azimuthal angle approaches bisector [30° in Fig. 1(a)] or perpendicular to bisector [120° in Fig. 1(b)]. As a matter of fact, we should use Eq. (9) to determine the azimuthal angles of the eigenmodes when the applied voltage is below or near threshold, and use Eq. (17) in the high-voltage regime. In the low-voltage regime, the LC molecules are uniformly twisted. On the other hand, in the high-voltage regime, the LC directors are aligned perpendicular to substrates except for the boundary layers. In an intermediate voltage, no simplified model is established and the azimuthal angle should lie between the extremes given by Eqs. (9) and (17). Also observed in Fig. 1, the azimuthal angle has a plateau in the vicinities of 0°, ±90°, and 180°, implying that the azimuthal angle is insensitive to $d\Delta n/\lambda$ in these regions. Between these watersheds, the azimuthal angle is rather sensitive to $d\Delta n/\lambda$. Moreover, this tendency becomes more prominent as $d\Delta n/\lambda$ increases. This is because when $d\Delta n/\lambda$ increases, the waveguiding effect becomes more prominent and the eigenmodes are either along or perpendicular to the *x*-axis, like those described in Eq. (8), except for some small vibrations between the two successive Gooch–Tarry minima conditions.[10]

III. SPECTRUM OF TN-LC-BASED FP ETALON

To investigate the eigenmodes of a reflective TN LC cell under different applied voltages, in the following we simulate the transmission spectrum of the TN-LC-based FP etalon. Without losing generality, we continue to choose the 60° TN LC cell as an example. In the simulations, we first use the continuum elastic theory[9] to calculate the director distributions and then use the 4×4 matrix method[14] to calculate the transmission spectra since the multiple reflections within the FP cavity must be considered. In our simulations, a commercial nematic mixture E-7 was used. The material parameters of E-7 are listed as follows: $\varepsilon_{\parallel}=19.6$, $\varepsilon_{\perp}=5.1$, $k_{11}=12\times10^{-12}$ N, $k_{22}=9\times10^{-12}$ N, $k_{33}=19.5\times10^{-12}$ N, and the refractive indices in the vicinity of $\lambda=1.5$ μm are $n_e=1.71$, and $n_o=1.50$.[15] The two inner surfaces of the FP cavity are assumed to have multilayer dielectric films[16] having 97% reflectivity.

A. Transmission spectra without voltage

Figure 2 shows the simulated transmission spectra of a 21-μm-thick, 60° TN-LC-based FP etalon without voltage. Three different incident conditions are considered: unpolarized light, linearly polarized light along *x*-axis ($P=0°$), and linearly polarized light perpendicular to *x*-axis ($P=90°$). For the unpolarized incident light, there are two eigenmodes in the FP etalon. While for the linearly polarized light, either parallel or perpendicular to the *x*-axis, only a single eigenmode resonates in the FP cavity. In addition, the spectra of the unpolarized incident light are the superposition of the two linearly polarized lights at $P=0°$ and $P=90°$. That means the eigenmodes of the FP cavity are the two linearly polarized lights parallel and perpendicular to the *x*-axis, which correspond to $d\Delta n/\lambda\sim3$ (i.e., 21 μm $\times0.21/1.5$ μm), as indicated in Figs. 1(a) and 1(b). Please notice that the result of $P=90°$ is equivalent to that of $P=-90°$ since the azimuthal angle has 180° periodicity.

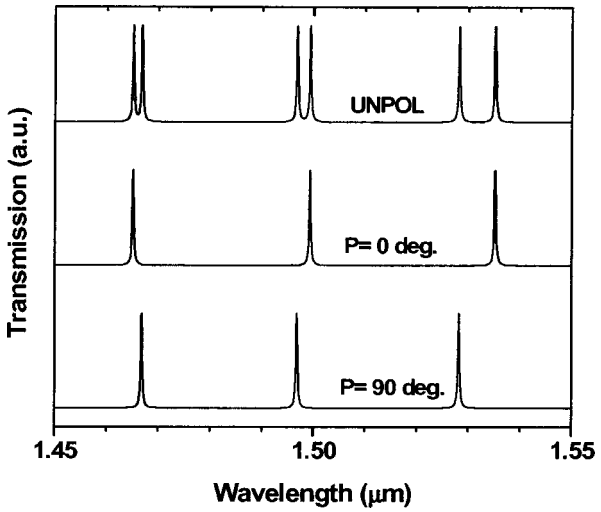

FIG. 2. The simulated transmission spectra of a 21-μm 60° TN-LC-based FP etalon without applied voltage. Three different incident light conditions are simulated: unpolarized light, linearly polarized light along the *x*-axis ($P=0°$), and linearly polarized light perpendicular to the *x*-axis ($P=90°$).

From Fig. 1, a small increase in the cell gap might cause a large change in the eigenmodes, depending on which regime is considered. We have calculated the transmission spectra of a 25-μm, 60° TN-LC-based FP cavity at $V=0$ for five different incident conditions: unpolarized light, linearly polarized light along the *x*-axis ($P=0°$), linearly polarized light perpendicular to the *x*-axis ($P=90°$), linearly polarized light at $P=-31°$, and linearly polarized light at $P=59°$. Results are depicted in Fig. 3. Similar to the case of 21-μm cavity, the spectra of the unpolarized incident light have two eigenmodes. However, the spectra for $P=0°$ and $P=90°$ also exhibit two modes in the 1.5-μm wavelength region. In these cases, the eigenmodes are no longer the linearly polarized lights parallel and perpendicular to the *x*-axis. For the spectra of $P=-31°$ and $P=59°$, only one mode occurs in the vicinity of $\lambda=1.5$ μm, while at other wavelengths, there are still two modes. Consequently, the two linear polarization states at $P=-31°$ and $P=59°$ are the eigenmodes only when the wavelength is close to 1.5 μm. The azimuthal angles of the eigenmodes will shift away from these two positions at other wavelengths. This phenomenon is evident from Figs. 1(a) and 1(b). In the region of $d\Delta n/\lambda\sim3.5$ (i.e., 25 μm$\times0.21/1.5$ μm) the azimuthal angles of the eigenmodes vary sharply with $d\Delta n/\lambda$. As a result, the mode coupling occurs at other wavelengths than 1.5 μm for the incident linearly polarized lights at $P=-31°$ and $P=59°$, as shown in Fig. 3. Even though the cell gap has already reached $d=25$ μm, the waveguiding condition is still imperfect. In fact, as $d\Delta n/\lambda$ increases further, the plateaus close to 0°, ±90°, and 180°, as shown in Fig. 1 become flatter, while the rising lines become sharper. Consequently, the azimuthal angle of eigenmodes under such condition is almost parallel or perpendicular to the *x*-axis, as discussed in Eq. (8).

B. Transmission spectra with voltage

Under applied voltage, the spectra in FP cavity generally shift to short wavelength due to the decrease of overall phase

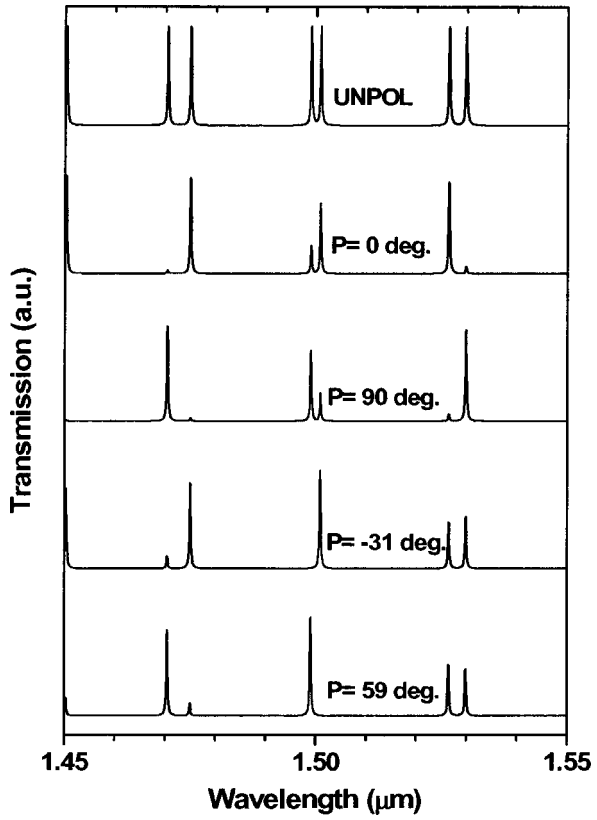

FIG. 3. The simulated transmission spectra of a 25-μm 60° TN-LC-based FP etalon without applied voltage. Five different incident light conditions are simulated: unpolarized light, linearly polarized lights along the *x*-axis ($P=0°$), perpendicular to the *x*-axis ($P=90°$), at $P=-31°$, and $P=59°$.

retardation. In this section, we choose two 60° TN-LC-based FP etalons with 21- and 1.5-μm cell gaps as examples to simulate the transmission spectra under various applied voltages.

Figure 4 plots the simulated transmission spectra of the 21-μm-thick, 60° TN-LC-based FP etalon at different incident polarization states. Figure 4(a) presents the results for the unpolarized incident light. Two sets of resonance peaks corresponding to two different eigenmodes are clearly observed. Figures 4(b) and 4(c) represent the cases of input linearly polarized light, with its polarization axis parallel ($P=0°$) and perpendicular ($P=90°$) to the *x*-axis. When the applied voltage is below threshold ($V_{th}\sim 0.8\ V_{rms}$), these two orthogonal linearly polarized lights are exactly the two eigenmodes in the FP cavity, as clearly seen by comparing Figs. 4(b) and 4(c) with 4(a). This is because the LC directors are not yet reoriented and the azimuthal angle of eigenmodes is along $P=0°$ [Fig. 1(a)] and $P=90°$ [Fig. 1(b), where $P=90°$ is equivalent to $P=-90°$ due to the 180° periodicity of azimuthal angle]. As the voltage increases to ~2 V, the LC molecules are slightly tilted and the effective birefringence decreases accordingly. Therefore, the azimuthal angle shifts slightly away from 0° and 90° as shown in Figs. 1(a) and 1(b). Hence, a small peak arises in addition to the main peak in each case as shown in Figs. 4(b) and 4(c). At the same time, the spectra peaks of $P=0°$ shift slightly towards shorter wavelengths, while the spectra peaks

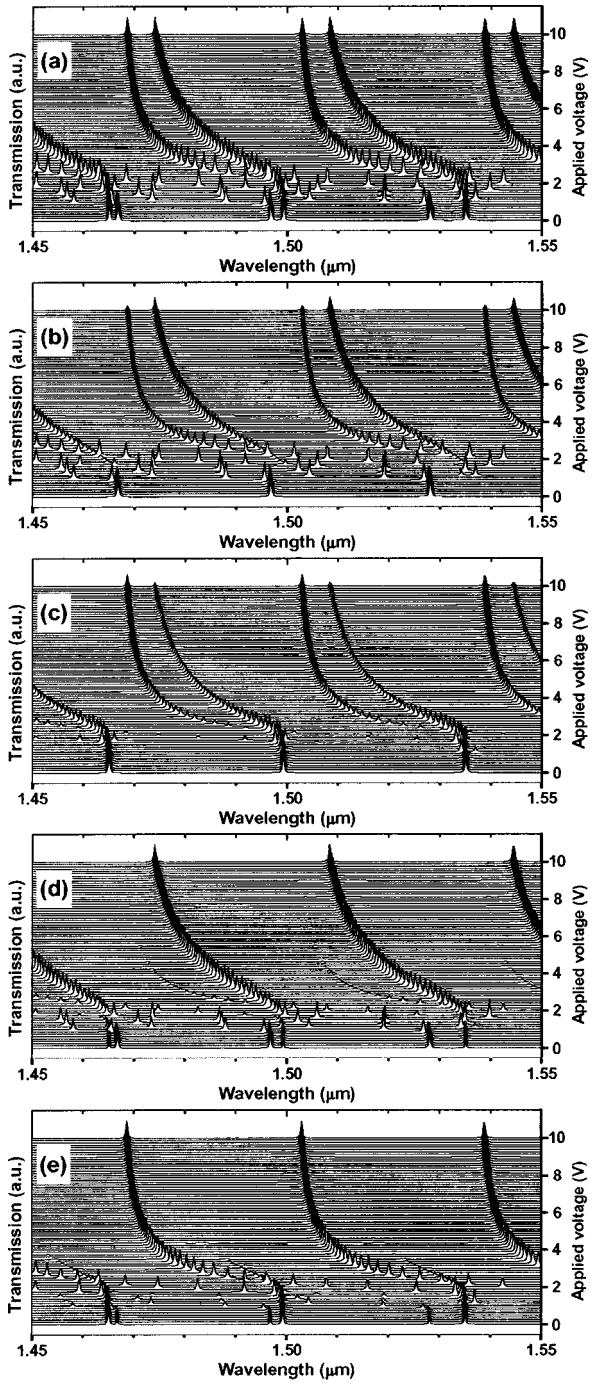

FIG. 4. The calculated optical transmission spectra of a 21-μm 60° TN-LC-based FP etalon at various applied voltages: (a) unpolarized incident light, (b) incident linearly polarized light parallel to *x*-axis ($P=0°$), (c) incident linearly polarized light perpendicular to *x*-axis ($P=90°$), (d) incident linearly polarized light parallel to the bisector of the twist angle ($P=30°$), and (e) incident linearly polarized light perpendicular to the bisector ($P=120°$).

of $P=90°$ almost keep unchanged since its effective refractive index is not significantly affected. As the applied voltage increases, the LC molecules are tilted further and the uniform twist structure of TN LC is broken. As a result, the azimuthal angles of eigenmodes change rapidly. Thus, two sets of resonance peaks for each incident linearly polarized light are produced.

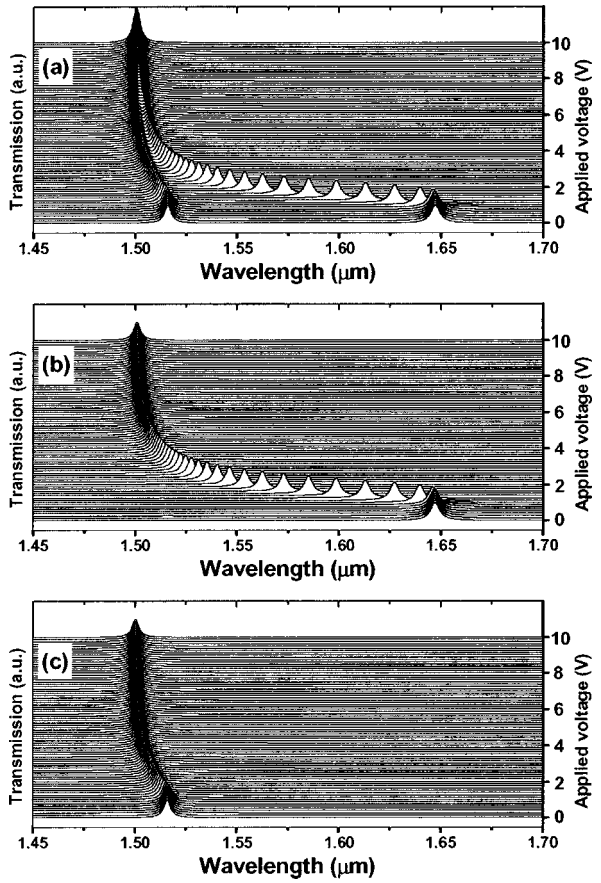

FIG. 5. The calculated optical transmission spectra of a 1.5-μm 60° TN-LC-based FP etalon at various applied voltages: (a) unpolarized incident light, (b) incident linearly polarized light parallel to the bisector of the twist angle ($P=30°$), and (c) incident linearly polarized light perpendicular to the bisector ($P=120°$).

Next, we consider the cases of the incident linearly polarized beams parallel and perpendicular to the bisector of twist angle. Figures 4(d) and 4(e) show the transmission spectra at $P=30°$ (i.e., $\phi/2$) and $P=120°$ (i.e., $\phi/2+\pi/2$), respectively. Their spectra are obviously different from those of $P=0°$ [Fig. 4(b)] and $P=90°$ [Fig. 4(c)]. In the low-voltage regime ($V<2$ V), there are two sets of resonance peaks since the azimuthal angles of eigenmodes are neither at $P=30°$ nor at $P=120°$. As the applied voltage exceeds $2\ V_{rms}$, one of the peaks gradually vanishes while the other gains intensity. Finally, as $V>6\ V_{rms}$, only one resonance peak exists in each case. This means under a very high voltage, the eigenmodes are those two linear polarization states parallel and perpendicular to the bisector. As predicted by the boundary layers model shown in Figs. 1(a) and 1(b), the azimuthal angles of eigenmodes approach the bisector or perpendicular to the bisector when $d\Delta n/\lambda$ approaches 0 in the high voltage regime. This phenomenon is so-called the bisector effect of a reflective TN LC cell.

The bisector effect phenomenon happens not only in the high-voltage state of a thick cell, but also in the voltage-off state of a very thin cell. Figure 5 depicts the simulated near-IR transmission spectra of a 1.5-μm-thick 60° TN-LC-based FP etalon under various voltages. Figure 5(a) represents the simulated results for an unpolarized incident light, while Figs. 5(b) and 5(c) are for the incident linearly polarized lights parallel and perpendicular, respectively, to the bisector. By comparing Figs. 5(b) and 5(c) with Fig. 5(a), we can clearly see that the spectra of the unpolarized light is exactly the linear superposition of those of linearly polarized light parallel and perpendicular to the bisector under any applied voltages. This indicates that even if no voltage is applied, the bisector effect is still clearly observed because of the small $d\Delta n$ value of the LC layer. The definition for a thin cell is that its half-phase difference ($\Gamma/2=\pi d\Delta n/\lambda$) is less than the twist angle ϕ. Of course, as voltage increases, $d\Delta n/\lambda$ further decreases and eventually approaches zero. According to the boundary layers model, the bisector effect would become more dominant if ψ gets closer to 0.

IV. CONCLUSIONS

The eigenmodes of the reflective TN LC cell are derived in details based on Jones matrix. Under zero or very low applied voltage, the uniform twist model is valid. On the other hand, in a very high voltage regime, the boundary layers model works well for the TN LC cell. The eigenmodes of a reflective TN LC cell are the two orthogonal linear polarization states. Moreover, these two eigenmodes are either parallel or perpendicular to the bisector when the phase retardation approaches 0 in a high-voltage state, or $\Gamma/2 \ll \phi$ at $V=0$. The eigenmodes are well investigated and proved by the transmission spectra of TN-LC-based FP etalons under various applied voltages. The accurate determination of eigenmodes in a reflective TN LC cell has two major impacts to the LC devices: (1) it will improve the contrast ratio of the direct-view and projection LC displays and (2) it will eliminate the resonance mode coupling of a TN-LC-based FP cavity for telecommunications applications.

ACKNOWLEDGMENTS

The authors would like to thank Professor Thomas X. Wu of UCF School of EECS for useful discussions concerning the simulation program. This work is supported by AFOSR under Contract No. F49620-01-1-0377.

[1] M. Schadt and W. Helfrich, Appl. Phys. Lett. **18**, 127 (1971).
[2] S. T. Wu and D. K. Yang, *Reflective Liquid Crystal Displays* (Wiley, New York, 2001).
[3] T. Sonehara, Jpn. J. Appl. Phys. **29**, L1231 (1990).
[4] S. T. Wu and C. S. Wu, Appl. Phys. Lett. **68**, 1455 (1996).
[5] K. H. Yang, *Proceedings of the 16th International Display Research Conference* Birmingham, England, 1996, pp. 449–452.
[6] H. A. Van Sprang, US Patent No. 5,490,003 (1996).
[7] J. S. Patel and S. D. Lee, Appl. Phys. Lett. **58**, 2491 (1991).
[8] P. Yeh and C. Gu, *Optics of Liquid Crystal Displays* (Wiley, New York, 1999).
[9] P. G. de Gennes and J. Prost, *The Physics of Liquid Crystals*, 2nd ed. (Clarendon, Oxford, 1993).
[10] C. H. Gooch and H. A. Tarry, J. Phys. D **8**, 1575 (1975).
[11] S. T. Wu and C. S. Wu, Jpn. J. Appl. Phys., Part 2 **37**, L1497 (1998).
[12] K. H. Fan Chiang, S. T. Wu, and S. H. Chen, Jpn. J. Appl. Phys., Part 1 **41**, 4577 (2002).
[13] J. S. Patel and Y. Silberberg, Opt. Lett. **16**, 1049 (1991).
[14] D. W. Berreman, J. Opt. Soc. Am. **62**, 502 (1972).
[15] S. T. Wu, Phys. Rev. A **33**, 1270 (1986).
[16] H. A. Macleod, *Thin-Film Optical Filters* (American Elsevier, New York, 1969).